Dynamics of Atmospheres and Oceans, 2 (1978) 107—122

A SIMULATION OF INERTIAL OSCILLATION IN DRIFTING PACK ICE

MILES G. McPHEE

AIDJEX — Division of Marine Resources, University of Washington, Seattle, Wash. 98195 (U.S.A.)

(Received June 17, 1977; accepted September 15, 1977)

ABSTRACT

McPhee, M.G., 1978. A simulation of inertial oscillation in drifting pack ice. Dyn. Atmos. Oceans, 2: 107—122.

A simple model for simulating the motion of pack ice during periods of energetic inertial oscillation is developed by writing an integrated momentum equation for the ice and upper ocean driven by surface wind stress. Damping is provided by a term proportional to the component of mass transport parallel to wind stress, which is a measure of the departure from a steady-state balance of wind stress and Coriolis force. Oceanic boundary-layer transport is taken to be proportional to the square of the surface velocity on the basis of extensive current measurements made under drifting ice, providing a relationship between ice velocity and total transport. Ice drift velocities measured at AIDJEX stations during the summer of 1975 are simulated with some success using measured local winds. A simple superposition of waves generated at the corners of the triangular array of stations is considered and it is shown that at times the waves are coherent across the 150 km array and at other times there is considerable interference at lesser scales. The importance of the motions for the production of new ice is briefly discussed.

INTRODUCTION

During the 1975—1976 AIDJEX (Arctic Ice Dynamics Joint Experiment) field project, an array of manned scientific stations was maintained for over a year on drifting ice floes in the Beaufort Gyre of the Arctic Ocean. The success of the experiment, which accurately measured ice and upper ocean response to surface winds, will greatly enhance our understanding of the coupled dynamic and thermodynamic processes that control the thickness and extent of the ice cover and will hopefully add a significant amount to our general knowledge of ocean—atmosphere interaction. The floes supporting the stations were an integral part of the pack (in contrast, e.g., to ice islands like T-3) and thus provided platforms for oceanographic work that are noteworthy in that their drift velocity was identical to the surface velocity of the ocean and they allowed to representative currents in the upper layer to be measured with relative ease.

A dominant feature of ice station motion during late summer of 1975 was a high level of inertial-period activity, manifested as cycloidal loops in drift trajectories measured by accurate navigational equipment, and as large-amplitude waves in velocity records of current meters positioned near the base of the mixed layer. Hunkins (1967) inferred similar motions in the drift of Fletcher's Ice Island (T-3) by considering speeds measured with deep current meters, and showed qualitatively how they would be generated by the observed winds. Indirect evidence of inertial ice motion may also be found in persistent accounts by early explorers of "tidal" periods in ice deformation, with alternate pressure ridging and lead opening.

From the point of view of ice dynamics, an important question is what effect the velocity waves have on longer-term properties of ice. The problem is that the conventional approach to modeling water stress in dynamical calculations of ice drift, i.e., expressing the drag directly in terms of ice velocity relative to the ocean, fails to allow the observed short-period motion because of inherent frictional damping. We would like to know how the inertia of the water column might be included in ice dynamics calculations in a way simple enough to be useful in a regional model of the ice pack. In this paper, we address the question by proposing a simple extension of the quadratic water drag formulation currently used in the AIDJEX ice model, and show that we can successfully simulate the observed motion including the inertial component.

Inertial oscillations superimposed on mean wind-drift currents in the upper layers of the open ocean were first discussed by Ekman (1905) and are by now well documented. Pollard and Millard (1970), hereafter referenced PM, simulated inertial velocity waves measured near the surface by modeling a simple system with wind stress distributed as a uniform body force in the mixed layer. Gonella (1971) reported observations of inertial waves excited by surface winds at depths of 10 m and 20 m in the Mediterranean. More recently, Kundu (1976) has analyzed inertial currents at several levels in the surface layer over the Oregon continental shelf, and found them to be, for the most part, wind driven.

While the main objective here is to investigate the transfer of momentum from the wind through the ice to the water as manifested by the ice velocity, we point out that the oceanic boundary-layer treatment, although simple, is founded on extensive measurements under drifting pack ice reported by McPhee and Smith (1976), henceforth called MS, and that it represents a significant departure from previous inertial-wave simulations.

DATA

Fig. 1 shows the configuration of the AIDJEX array representative of times when strong inertial motions were present in the ice station trajectories. The manned camps (*BB*, *CA*, *BF*, and *SB*) formed a triangle centered roughly 600 km northeast of Barrow, Alaska. The other designations (*R* and

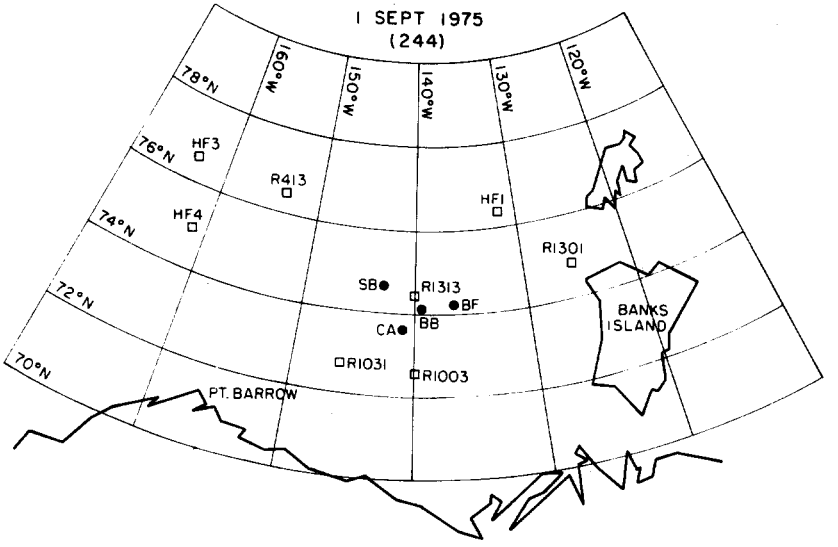

Fig. 1. Locations of AIDJEX manned ice stations (*BB*, *CA*, *BF*, *SB*) and unmanned data buoys (*HF* and *R* prefixes) on 1 September 1975.

HF) indicate unmanned data buoys measuring surface pressure, air temperature and position.

Winds were measured at the manned camps with fast-response cup anemometers and wind vanes mounted 10 m above the surface. In addition, a 25-m tower at the central main camp Big Bear (*BB*) furnished wind profile and direct turbulence data allowing accurate determination of 10-m drag coefficients. An independent check on the stress data was provided at each of the camps by an analog filtering technique applied to the anemometer data to estimate the turbulent dissipation.

Station positions were determined by Doppler satellite navigation (NavSat) from as many as 30 fixes per day, each with absolute geographical accuracy of about 40 m. The data were processed for AIDJEX purposes using Kalman smoothing techniques (Thorndike and Cheung, 1977), yielding equally spaced (3-hour) time series of position, velocity, and acceleration. Unfortunately, even with maximum sampling frequency, the present configuration of the filter attenuates part of the power at the inertial period (12.4 hours at 75°N). This, combined with the non-uniform nature of the sampling, prompted us to look to the current measurements for a more reliable definition of the short-period motion.

Currents were measured from the manned camps at 2 m and 30 m below the ice undersurface. Speed and streamline bearing of flow relative to the moving ice were sampled continuously at 30-sec intervals. It is important to note that in a frame of reference drifting with the ice one sees small currents near the surface increasing to some "free stream" velocity in the interior, while in a fixed-to-earth frame currents are small except within a few

meters of the surface. In the absence of horizontal density gradients in the boundary layer, the vector sum of this free stream velocity and the absolute ice velocity is the geostrophic current, $\vec{V}_g$, due to sea-surface slope. If changes in $\vec{V}_g$ are slow compared with time scales of interest, it is appropriate to think of the whole wind-drift regime as being advected passively by $\vec{V}_g$. Thus, in principle, the ice motion due to wind stress is best found by measuring the shear between the ice and the water at some level in the mixed layer below which the effects of surface stress are vanishingly small. In practice, this shear is estimated from the measured current at 30 m.

A reference level at 30 m was chosen for the fixed current meters under the AIDJEX array as a compromise between the maximum depth of frictional influence observed during the 1972 pilot study (~35 m) and the depth of the expected summer mixed layer (~25 m). Final density data from the 1975—1976 experiment are not yet available, but preliminary analysis indicates that fresh melt water accumulating near the surface in calm weather is rapidly mixed down into a homogeneous layer extending to the top of the main halocline at 25—30 m when ice motion is strong (K. Hunkins, personal communication). As freeze-up progressed the mixed layer gradually deepened until it reached a depth of 40—50 m in late winter.

In addition to the geostrophic flow argument given above, the practical reasons behind using the shear between the ice and the 30-m level to estimate the inertial motion of the ice are demonstrated by Figs. 2a and b. Each graph shows one component of ice velocity measured with respect to three references. The top trace is the absolute ice velocity as obtained from the smoothed NavSat navigational fixes; the middle trace is the velocity with respect to the 30-m level using hourly averages from the current meter suspended there; and the bottom trace is the ice velocity with respect to a cur-

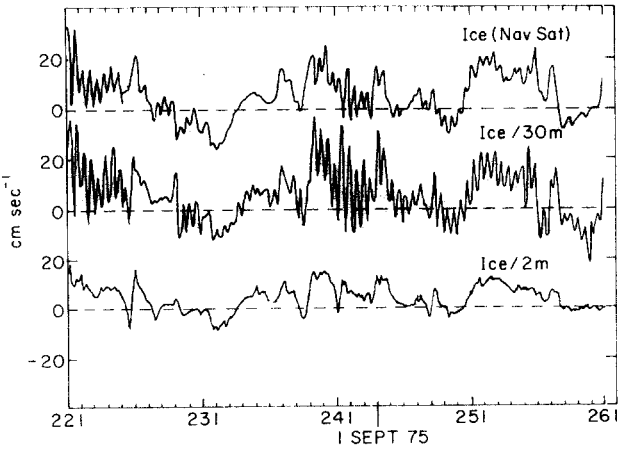

Fig. 2a. Zonal (east positive) velocity component of the ice measured by navigation (top); with respect to the 30-m level in the ocean (middle); and with respect to the 2-m level (bottom), 9 August 1975 to 18 September 1975.

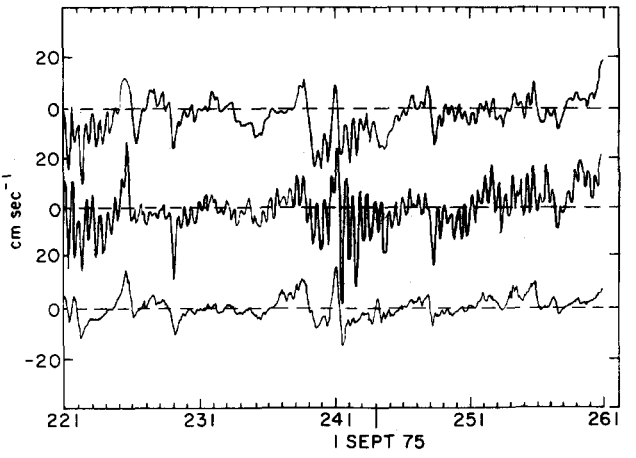

Fig. 2b. Same as Fig. 2a except meridional (north positive) component.

rent meter at 2 m. During the first few days of the record the number of good navigational fixes was sufficient to define the oscillations quite well, and most of the difference between the top and middle traces is probably due to attenuation by the Kalman filter. Beginning about day 225 there is a gap in the NavSat data which has the effect of smoothing over the abrupt change apparent in the current meter records on day 226. The smoothing of the NavSat record after day 235 also coincides with a falloff in the frequency of good satellite fixes.

The relative steadiness of the ice/2 m velocity indicates that the water col-

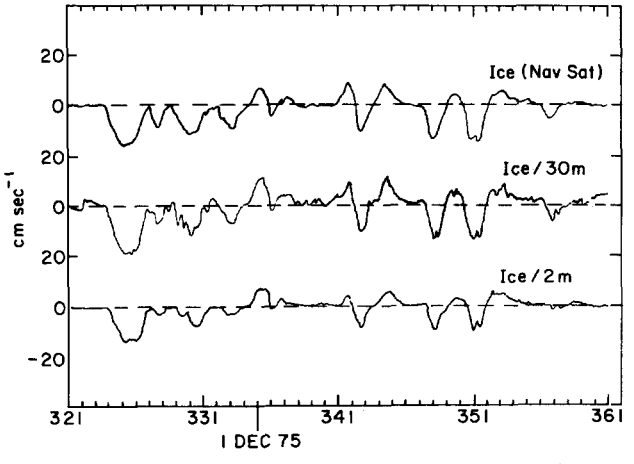

Fig. 3. Zonal component of ice velocity relative to three references during winter, 17 November 1975 to 27 December 1975.

umn at 2 m is oscillating in phase with the ice with almost as much amplitude in spite of fairly large mean shear in the "wall" layer between the ice and 2 m.

Fig. 3 shows a similar comparison for the zonal component at station Caribou in early winter when the ice was more compact but still relatively mobile. Strong damping of inertial waves by the ice cover is readily apparent, and the close correspondence between the NavSat and ice/30 m traces shows the absence of appreciable wind-drift current at 30 m. If the velocity series in Fig. 2 are low-pass filtered at 12 hours, the result is qualitatively similar to Fig. 3.

THE MODEL

The physics of the model is best described by considering a homogeneous, quiescent ocean overlain by an ice pack of uniform thickness, h, and density, ρ_i. If we neglect any stress gradient imposed on the ice from distant boundaries, the only driving force is the wind, which is assumed to be spatially uniform so that no horizontal gradients exist in the problem. The momentum equation for any element in the ice—ocean system may then be written:

$$\rho\left(\frac{\partial \vec{v}}{\partial t} + f\hat{k} \times \vec{v}\right) = \frac{\partial \vec{\tau}(z)}{\partial z}$$

where $f\hat{k}$ is twice the vertical component of the earth's rotation rate and $\vec{\tau}(z)$ is the horizontal traction at any level, z. With the origin at the ice—ocean interface, the momentum equation can be integrated up or down to yield:

$$\text{Ice:} \quad \rho_i h\left(\frac{\partial \vec{V}}{\partial t} + f\hat{k} \times \vec{V}\right) = \vec{\tau}_s - \vec{\tau}(0) \tag{1}$$

$$\text{Water:} \quad \rho_w \int_{-H}^{0} \left(\frac{\partial \vec{U}(z)}{\partial t} + f\hat{k} \times \vec{U}(z)\right) dz = \vec{\tau}(0) \tag{2}$$

where $\vec{\tau}_s$ is the surface wind stress; H is an arbitrary depth chosen so that the turbulent stress at that level is always vanishingly small; $\vec{V}$ is the velocity of the rigid ice column; and $\vec{U}(z)$ is the depth-varying velocity in the water column. We define $\vec{M}_w$ as the net mass transport in the upper ocean:

$$\vec{M}_w = \int_{-H}^{0} \rho_w \vec{U}(z) dz$$

and seek to couple oceanic transport to the ice momentum by considering the structure of currents measured at AIDJEX camp Jumpsuit in April, 1972.

Fig. 4, from data in MS, shows current profiles relative to the 32-m level on successive days of the 1972 experiment. The x-axis is in the direction of

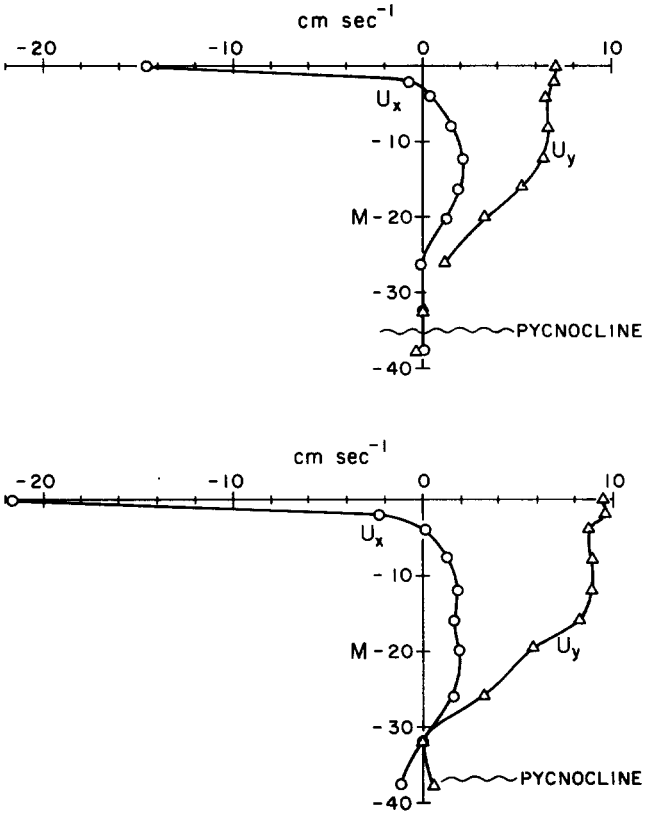

Fig. 4. Current profiles measured from drifting pack ice at the 1972 AIDJEX pilot study camp. Top: 8 hour average, 11 April 1972. Bottom: 5 hour average, 12 April 1972.

interfacial stress. Over the averaging time the profiles changed very little, allowing the turbulent structure to approach a steady state. Under these conditions, (2) requires mean transport to be to the right of surface stress. This is borne out well by the measurements: the net transport is essentially the area under the U_y profile despite large shear in the U_x component near the surface. Note that the depth to which the surface-driven currents penetrate increases with increasing speed and in neither case do the profiles fill the entire mixed layer.

A significant result from the 1972 study (MS) was that measurements of boundary-layer turbulence agreed reasonably well with a class of atmospheric boundary-layer models (e.g., Wyngaard et al., 1974; and Businger and Arya, 1974) for which the scaling with neutral stability is u_* for velocity and some fraction of u_*/f for depth, where u_* is the surface-layer turbulent scaling velocity. Over the limited range of Rossby numbers encountered under drifting ice, we expect u_* to vary as V, and the turning angle, β, to be

nearly constant. The similarity of dimensionless profiles found in 1972 thus implies that the dimensional area under the lateral profile (U_y in Fig. 4b) is proportional to V^2/f. Geometrically this is clear if one considers the lateral profile to be roughly triangular with one leg equal to $V \sin \beta$ and the other proportional to V/f. Both our measurements and the models mentioned above suggest that the lateral profile of velocity (perpendicular to surface stress) more closely resembles a linear decrease from the surface value to zero than a "slab" with large shear at the base as suggested, e.g., by PM.

By choosing a suitable proportionality constant, c_w, the steady-state transport vector in the boundary layer can be expressed in terms of ice velocity as:

$$\vec{M}_w = -\rho_w c_w \frac{V}{f} \hat{k} \times \vec{V} \cdot \underset{\sim}{B} \tag{3}$$

where $V = |\vec{V}|$ and $\underset{\sim}{B}$ is a rotation operator:

$$\underset{\sim}{B} = \begin{bmatrix} \cos\beta & -\sin\beta \\ \sin\beta & \cos\beta \end{bmatrix}$$

Substitution of (3) into (2) shows that for *steady* conditions the magnitude of the interfacial stress is:

$$|\vec{\tau}(0)| = \rho_w c_w V^2$$

and is directed at an angle $\pi - \beta$ clockwise from $\vec{V}$. This is the form of the water stress term in the AIDJEX ice model, except that $\vec{V}$ is replaced by an ice velocity relative to undisturbed geostrophic flow in the ocean. In the free-drift version of the ice model where horizontal gradients are neglected, the local time derivative term in (2) is ignored and (1) is solved directly using a prescribed wind stress. From this it is clear that the inertia of the water column is excluded in the ice model calculations.

In order to generalize the water drag law to include the missing inertia, we consider the total mass transport of the system:

$$\vec{M} = \rho_i h \vec{V} + \vec{M}_w$$

$$= \rho_i h \vec{V} - \rho_w c_w \frac{V}{f} \hat{k} \times \vec{V} \cdot \underset{\sim}{B} \tag{4}$$

and the sum of eqs. 1 and 2:

$$\frac{d\vec{M}}{dt} + f\hat{k} \times \vec{M} = \vec{\tau}_s$$

This is physically unrealistic, because the idealization implied in (4) has eliminated any dissipative process necessary for damping oscillations (this can be seen by considering the response after cessation of a steady wind). For the simple inertial model, we postulate a damping force, $\vec{F}_d$, of the

form:

$$\vec{F}_d = -\frac{d_0 f}{2\pi} \frac{(\vec{M} \cdot \vec{\tau}_s)}{|\vec{\tau}_s|^2} \vec{\tau}_s \tag{5}$$

Although this term may appear cumbersome, it is the simplest consistent with the following reasoning. The main factor in the suppression of the waves seems to be the stiffness or compactness of the ice. During winter and spring, the ice is quite effective at quelling oscillation even though we often see times when its mean drift appears to reflect an approximate balance among air stress, Coriolis force and water stress. A plausible physical explanation is that the scale over which the inertial motions are coherent is considerably less than the scale of the major atmospheric disturbance causing mean motion, so that even though a whole region of ice moves with little apparent resistance, internal forces at smaller scales in the compact winter pack rapidly quell the inertial component. Therefore, in a locally driven model we would like an expression that can provide strong damping, yet still allow a steady state:

$$\rho_i h f \hat{k} \times \vec{V} = \vec{\tau}_s - \vec{\tau}(0)$$

Thus, we make the damping proportional to departure from steady state, a measure of which is given by the component of transport antiparallel to the wind stress. This allows direct comparison between models with or without the oceanic inertia.

The inertial model therefore consists of integrating numerically the equation:

$$\frac{d\vec{M}}{dt} + f\hat{k} \times \vec{M} = \vec{\tau}_s + \vec{F}_d \tag{6}$$

for an observed wind stress, and then obtaining $\vec{V}$ from $\vec{M}$ using (4). Note the implicit assumption that the boundary layer is "locked" in phase with the ice. The rationale is that the time scale of the turbulent eddies providing the momentum transfer is short compared to the inertial period, and thus the boundary layer adjusts quickly to the changing velocity at the surface. This assumption, of course, is only an approximation, but is necessary for simplicity and gains support from the absence of large inertial components in currents measured relative to the ice at 2 m (Fig. 2).

Eq. 6 is seemingly similar to the model proposed by PM, and also used by Kundu (1976) to simulate currents measured near the surface from a fixed mooring. The differences are instructive, however. First, PM use linear damping, i.e., in our notation:

$$\vec{F}_d = -c\vec{M}$$

which seems a reasonable approach in the open ocean, but does not address a highly dampening ice cover as discussed above. A few numerical experiments showed that the difference between calculating transport with this linear

damping as opposed to (5) is not particularly significant when the damping is small. The major distinction between the two models lies in their treatment of the velocity distribution in the boundary layer. As mentioned before, PM postulate a "slab" boundary layer of depth H, corresponding to the mixed layer depth, so that:

$$\vec{M} = H\vec{U}$$

We found that a slab model could not meet the criteria imposed by our data. Obviously, the surface velocity, which would be the ice velocity in our case, is not perpendicular to surface stress in a steady state, and one presumes that PM were neglecting a constant-stress surface layer as is often done when Ekman (constant K) theory is invoked (e.g., see Hunkins, 1966). More important, however, is the fact already mentioned, that the 1972 measurements showed the frictional boundary layer to scale with u_*/f, not with the depth of the mixed layer, and that in general there was not much mean shear at the base of the mixed layer (MS).

Evidence against the slab concept is also found in well-documented observations (e.g., see Browne and Crary, 1958) that the water stress (averaged over inertial cycles) acting on pack ice varies as the square of the ice velocity relative to the undisturbed ocean. If the depth, H, proposed by PM is constant or slowly varying, then the transport and therefore the steady state stress is approximately linear in V. In terms of surface stress (and velocity), this is similar to the classical Ekman treatment with constant eddy viscosity, i.e., surface stress proportional to V rather than V^2. Since shear at the interface between the mixed layer and the pycnocline is often invoked as an important mechanism for mixed-layer growth (Pollard et al., 1973; Niiler, 1975), this raises a significant point. A slab model will provide shear at the density interface any time there is motion; by contrast, a model like the one here with frictional depth dependent on V/f imposes an additional, often severe, constraint on the mean current profile.

The effects of stratification near the surface, which is often present in the summer due to melting ice, have been neglected because it is thought that the water column down to the main halocline will become well mixed during the first cycle of a strong inertial episode and thereafter remain neutral. Of course, it is possible that at times the velocity dependent boundary layer depth will exceed the mixed layer depth. Such occurrences are of much interest in other contexts such as mixed layer growth, but it is hard to see how they could have a major effect on the surface (ice) velocity.

The important features of the model are: (1) the total transport is proportional and perpendicular to the surface stress in a steady state; (2) damping in the system depends in a simple way on the departure from steady state; and (3) the transport in the water column varies as the square of the ice (surface) velocity since the depth of frictional penetration is proportional to V/f.

SIMULATIONS

The wind-drift motion at the manned camps was simulated using surface wind stress calculated from wind measured at 10 m according to:

$$\vec{\tau}_s = \rho_a c_{10} |U_{10}| \vec{U}_{10}$$

where ρ_a is the air density, and $c_{10} = 0.0027$, which includes an estimate of increased drag due to pressure ridges (E. Leavitt, personal communication). Stress components during a 20-day period at station Caribou (*CA*) are shown in Fig. 5.

The corresponding ice velocity relative to 30 m is shown by the top traces of Figs. 6a and b. For comparison purposes, a simulation was first done with a passive water drag, i.e., eqn. 1 solved with:

$$\vec{\tau}(0) = \rho_w c_w |\vec{V}| \vec{V} \cdot \underset{\sim}{B}$$

with $\rho_w = 1.0$; $c_w = 0.0055$, and $\underset{\sim}{B} = 23°$, where these drag parameters were chosen from consideration of drift trajectories in the summer. The ice mass was taken to be 300 g/cm^2. Results are shown as the middle traces. Except for a small offset due to geostrophic ocean flow (<2 cm/sec), this is what would be predicted by the AIDJEX pack ice model, since zero ice strength at this time of year would make the momentum balance essentially local. Note that although the mean trend is well represented, the inertial component is badly underestimated as discussed above.

The results of a simulation in which the oceanic inertia was retained as suggested in the previous section are shown in the bottom traces of Figs. 6a and b for the same values of β and c_w with $d_0 = 1.0$. Clearly the inertial am-

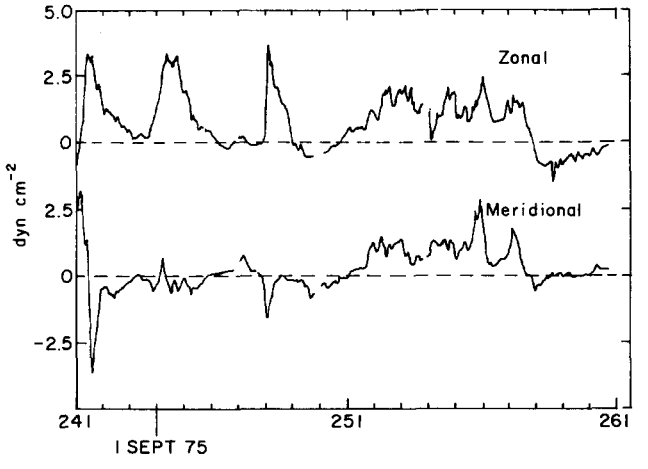

Fig. 5. Components of surface air stress at station Caribou, 29 August 1975 to 18 September 1975.

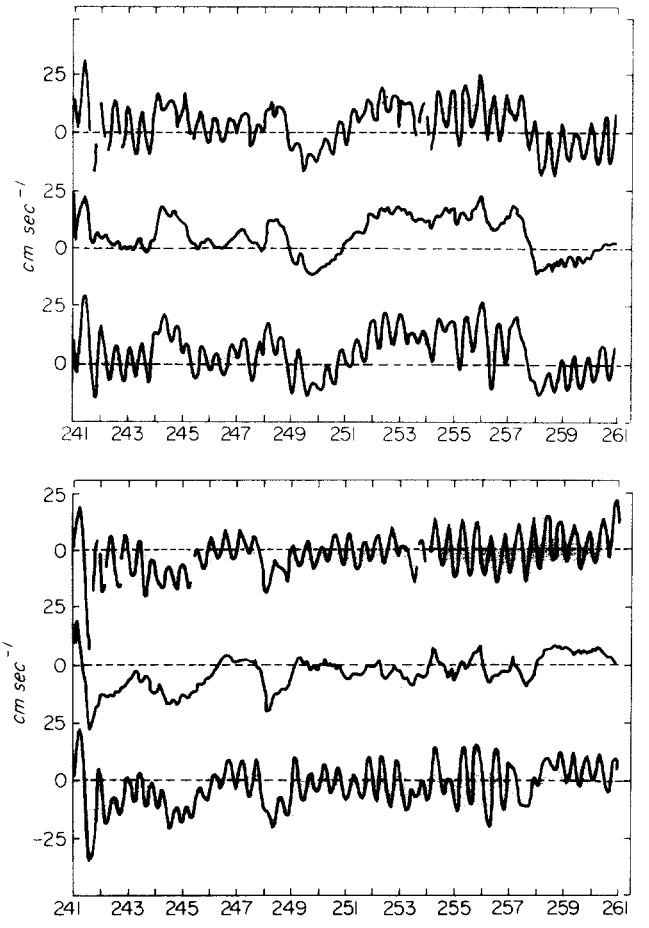

Fig. 6a. Zonal component of ice velocity at station Caribou. Top trace: observed with respect to 30 m; middle: simulation with passive quadratic water drag; bottom: simulated with inertial model.
Fig. 6b. Same as Fig. 6a except meridional component.

plitude is much better modeled than with the passive drag, and although the damping appears somewhat strong at times (e.g., days 241—244) and there are other times when the signals drift out of phase, the overall correspondence is remarkable considering the crudeness of the boundary-layer treatment.

An obvious question arises when one considers how the inertial motions are generated: what is the effect of spatial gradients in the wind field? In spite of the fact that horizontal homogeneity was assumed in the derivation, the configuration of the AIDJEX array may allow us to draw some useful conclusions about the pertinent space scales of the motions. The idea is to look at a simple superposition of velocity waves generated by the winds ob-

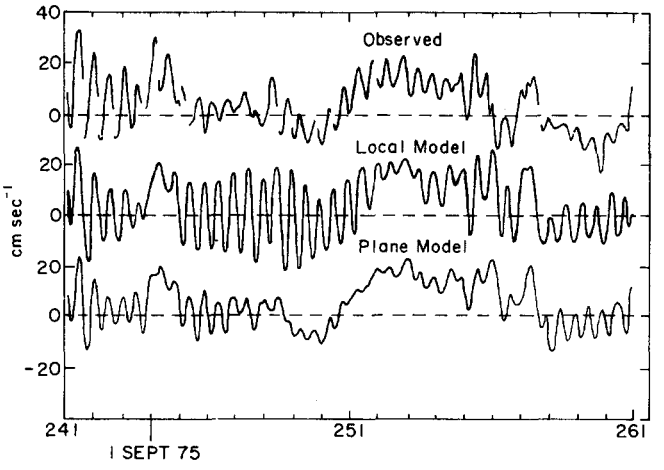

Fig. 7. Zonal velocity of central station Big Bear. Top trace: observed; middle: inertial model driven with local wind; bottom: plane superposition of simulations driven at outer stations.

served at the three corners of the array (*CA*, *BF*, *SB* — see Fig. 1) and compare them with the observed velocity waves at the central camp and also with waves predicted from the central camp wind. Thus, if a particular wind event forces oscillations of equal strength at the corners simultaneously, the local response should follow closely the regional response. On the other hand, if the excitation is out of phase across the array, there may be appreciable interference at a point within the triangle.

A calculation along these lines is shown in Fig. 7 for the zonal component of ice velocity at the central camp Big Bear. The top trace shows the observed ice/30 m velocity. The second trace is for a simulation using the observed wind at Big Bear with the same parameters used in the Caribou run. The bottom trace in Fig. 7 is the result of the procedure described above: simulations were run using winds observed at the three corner camps (the bottom trace of Fig. 6a is the example for Caribou); then the calculated velocity component and the coordinates of each camp were used to evaluate the coefficients A, B, and C such that

$$u_E = Ax + By + C$$

where x, y are coordinates in the horizontal plane of the camps. The velocity at Big Bear was then found from this superposition using its coordinates.

For the first few days the local model reproduces the observed waves well enough, but then beginning about day 245 the predicted amplitude is larger than observed implying that the local response is being affected by nonhomogeneous processes. During the period 245—251 it is clear that there is interference across the array, and in fact, the superposition of waves generated at three points from 50 to 120 km distant produces a better approx-

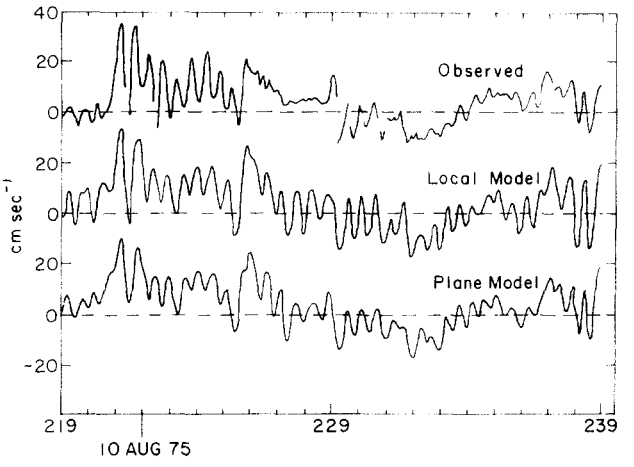

Fig. 8. Same as Fig. 7, except for period 9 August 1975 to 29 August 1975.

imation to the observed amplitudes than does the local wind. During the first few days, it appears as if the whole region is moving in phase with roughly the same amplitude. Fig 8 is identical to Fig. 7 except for an earlier time period. During the last half of the period, the superposition appears closer to the observed, but during the period 226—229, neither simulation shows the strong damping seen in the ice/30 m measurement. This might be due to a temporary tightening of the ice pack around Big Bear.

DISCUSSION

Data shown here indicate that for periods less than a day, the inertia of the moving water in the ice—ocean boundary layer is an important part of the total surface momentum balance. By using a simple momentum equation in which the mass transport in the oceanic boundary layer is proportional to the square of the surface velocity, we have simulated inertial waves in ice drift velocity with some success.

An elementary superposition of response to winds observed at the corners of the AIDJEX array suggests that at times the oscillations are coherent across scales of at least 150 km, while at other times there may be appreciable interference due to horizontal variations in the wind at lesser scales. One implication of this is that the inertial motions could be a major factor in the production of new ice during the fall, since zones of alternate divergence and convergence would tend to first expose open water to rapid freezing, then compress the newly formed ice in pressure ridges. What Nansen described as "tidal" oscillations in pressure against the hull of the *Fram* during October, 1893, may have been such an event (e.g., see his diary excerpts in Nansen, 1968). A more thorough investigation of the spatial variation and coherence

of ice station motion during inertial episodes using AIDJEX data is planned.

The transition in inertial response from summer to winter is striking. Apparently as freeze-up progresses, the ice becomes rigid on a large enough scale to inhibit the short-period motion almost entirely. Thus the ice—ocean boundary layer takes on two distinct characters depending on the season. In winter, the ice is essentially a "rigid lid", and the boundary layer as measured in a frame of reference drifting with the ice is a direct analogue of the atmospheric boundary layer. During summer, there is still a no-slip condition between ice and water but the ice is no longer constrained in the horizontal and the boundary layer is presumably more like that of the open ocean, except that surface waves are absent. Work now in progress indicates that the magnitude and direction of net ice drift over several inertial periods is not particularly sensitive to the level of inertial activity, suggesting that nonlinear effects of the waves on the mean flow profiles are small. If one could show this conclusively, perhaps by making comprehensive upper ocean measurements during summer when the ice is freely oscillating to be compared to similar measurements already made under nearly steady conditions (MS), it might be very helpful in bridging the gaps between oceanic and atmospheric boundary layer theory and increasing our general knowledge of momentum transfer between the two fluids.

ACKNOWLEDGMENTS

I am indebted to many of my colleagues at AIDJEX, particularly F. Carsey, R. Colony, E. Leavitt, D. Rothrock and A.Thorndike, for helpful discussion about these features and for aid in amassing the data with which to drive and verify the model. This work was supported by the National Science Foundation under grant OPP71-04031 and by AIDJEX.

REFERENCES

Browne, I.M. and Crary, A.P., 1958. The movement of ice in the Arctic Ocean. In: Arctic Sea Ice. NAS-NRC Publ. No. 598, pp. 191—208.

Businger, J.A., and Arya, S.P.S., 1974. The height of the mixed layer in the stably stratified planetary boundary layer. In: Advances in Geophysics, 18A. Academic Press, New York, N.Y., pp. 73—92.

Ekman, V.W., 1905. On the influence of the earth's rotation on ocean currents. Ark. Mat. Astron. Fys., 2 (11).

Gonella, J., 1971. A local study of inertial oscillations in the upper layers of the ocean. Deep-Sea Res., 18: 775—778.

Hunkins, K., 1966. Ekman drift currents in the Arctic Ocean. Deep-Sea Res., 13: 607—620.

Hunkins, K., 1967. Inertial oscillations of Fletcher's Ice Island (T-3). J. Geophys. Res., 72: 1165—1174.

Kundu, P.K., 1976. An analysis of inertial oscillations observed near the Oregon coast. J. Phys. Oceanogr., 6: 894—908.

McPhee, M.G. and Smith, J.D., 1976. Measurements of the turbulent boundary layer under pack ice. J. Phys. Oceanogr., 6: 696—711.

Nansen, F., 1968. Adrift on the polar seas. In: S. Manley and G. Lewis (Editors), Polar Secrets: A Treasury of the Arctic and Antarctic. Doubleday, Garden City, New York, N.Y., pp. 186—222.

Niiler, P.P., 1975. Deepening of the wind-mixed layer. J. Mar. Res., 33: 405—422.

Pollard, R.T. and Millard Jr., R.C., 1970. Comparisons between observed and simulated inertial oscillations. Deep-Sea Res., 17: 813—821.

Pollard, R.T., Rhines, P.B. and Thompson, R.O.R.Y., 1973. The deepening of the wind-mixed layer. Geophys. Fluid Dyn., 3: 381—404.

Thorndike, A.S. and Cheung, J.Y., 1977. AIDJEX measurements of sea ice motion: 11 April 1975 to 14 May 1976. AIDJEX Bull., 35: 1—149.

Wyngaard, J.C., Cote, O.R. and Rao, K.S., 1974. Modeling the atmospheric boundary layer. In: Advances in Geophysics, 18A. Academic Press, New York, N.Y., pp. 193—212.